Nuclear Instruments and Methods in Physics Research A 694 (2012) 162–166

Contents lists available at SciVerse ScienceDirect

Nuclear Instruments and Methods in Physics Research A

journal homepage: www.elsevier.com/locate/nima

Secondary effects on electron multiplication in pure isobutane

A. Mangiarotti [a,b], I.B. Lima [c], T.C. Vivaldini [c], J.A.C. Gonçalves [c,d], A.R. Petri [c], S. Botelho [c,d], P. Fonte [a,e], C.C. Bueno [c,d,*]

[a] Laboratório de Instrumentação e Física Experimental de Partículas, Departamento de Física da Universidade de Coimbra, 3004-516 Coimbra, Portugal
[b] Departamento de Física, Faculdade de Ciências e Tecnologia, Universidade de Coimbra, Coimbra, Portugal
[c] Instituto de Pesquisas Energéticas e Nucleares, 05508-000 Cidade Universitária, São Paulo, Brazil
[d] Departamento de Física, Pontifícia Universidade Católica de São Paulo, 01303-050 São Paulo, Brazil
[e] Instituto Superior de Engenharia de Coimbra, 3030-199 Coimbra, Portugal

ARTICLE INFO

Article history:
Received 5 June 2012
Received in revised form
6 August 2012
Accepted 7 August 2012
Available online 16 August 2012

Keywords:
Electron transport parameters
First Townsend coefficient
Isobutane
Space charge
Ohmic drop

ABSTRACT

The presence of secondary processes in electron multiplication under high uniform electric fields at atmospheric pressure in pure isobutane was investigated. The experimental setup consists of a Resistive Plate Chamber-like cell with the anode made of a high resistivity glass ($2 \times 10^{12}\ \Omega$ cm) and a metallic cathode, on which photoelectrons are produced by the incidence of a pulsed laser beam. In particular, the dependence of the first Townsend coefficient (α) on the repetition rate and the intensity of the UV laser pulses was studied. The E/N range considered spanned from $\approx$145 to $\approx$200 Td. The α coefficient was determined by measuring both the primary ionization and the avalanche currents with the help of an electrometer, directly connected to the cathode. Of all the investigated secondary effects, only the ohmic drop across the resistive glass has been found to be non-negligible in the present experimental conditions and has been corrected for. The obtained values are compared with Magboltz simulation results and presented in tabular form.

1. Introduction

The knowledge of electron transport parameters in gases (mostly drift velocity and first Townsend coefficient) is an important aid in designing gaseous detectors from proportional counters to novel micro-structures. Moreover, they can be used to constrain electron impact cross-sections, relevant in other very different areas of physics, as in the control of plasma assisted processing, where discharges in gases are involved. With this broad-band of application in mind, our group built and commissioned a dedicated setup to experimentally investigate electron transport in gases [1], on which a first round of improvements has recently been completed concerning laser focussing problems and field non uniformities [2].

The most important results obtained so far concern isobutane, a commonly used filling gas in several detectors and a component of a tissue equivalent mixture for micro and nano dosimeters. The drift velocity was measured [1] well into the saturation region up to $E/N \approx 200$ Td ($1\ \text{Td} = 10^{-21}\ \text{V m}^2$) for the first time, employing the classical Townsend Time-of-Flight method. The first Townsend coefficient was better measured in our second paper [2], using the current gain in pulsed mode, covering the same electric field range, where no data were available before. To reach even higher values of E/N, some technical limitations remain, as well as the difficulty of employing the correct set of transport parameters, once the continuous (Steady State Townsend) and pulsed (Pulsed Townsend) regimes cannot be regarded as equivalent. Simulations performed with the Magboltz code indicated that high field effects on the electron multiplication kinetic, influencing the definition of the drift velocity and of the ionization rate, can be neglected in the range of field strengths considered here [3].

The measurements of electron multiplication in gases can be distorted by several effects, generally falling into two broad categories: effects produced by apparatus non idealities and unwanted physical processes. After having discussed the several improvements made to our setup [2], the present paper is instead dedicated to experimental investigations of the physical processes possibly present in our system. The focus is again on isobutane in view of the interesting results previously obtained. By adopting a parallel plate configuration, avalanche non equilibrium effects [4] around thin wires have been avoided all together.

The next section is devoted to a classification of the effects mentioned in the previous paragraph, showing how they can be disentangled using their dependence on E/N, on the laser pulse repetition rate and on the laser beam intensity. In the third

* Corresponding author at: Av. Lineu Prestes 2242, Cidade Universitária, 05508-000 São Paulo, SP, Brazil. Tel.: +55 1131339830; fax: +55 1131339765.
E-mail address: ccbueno@ipen.br (C.C. Bueno).

0168-9002/$ - see front matter © 2012 Elsevier B.V. All rights reserved.
http://dx.doi.org/10.1016/j.nima.2012.08.017

section the main features of the setup will be recalled and the results presented in the forth section. Finally, the results will be discussed and some conclusions will be drawn.

2. Secondary processes in uniform fields

Basically, in our setup, a uniform electric field is established by means of two parallel plane electrodes. Its peculiarity is the use of a Resistive Plate Chamber (RPC)-like structure with a glass covered anode to protect the system from sparks, since it is operated at atmospheric pressure. The electron cloud is started by shining a UV laser on the cathode and the fast induced signals (i.e. electronic) as well as the total integrated current (i.e. electronic plus ionic) are measured with a scope and an electrometer, respectively (further details will be given in Section 3). There are five physical processes which can possibly be present in the current conditions and will be investigated experimentally: (i) avalanche space charge effects produced by the ions left behind from previous pulses, (ii) avalanche space charge effects within a single electron cloud, (iii) effects of the ohmic drop in the resistive glass anode, (iv) recombination processes inside a single electron cloud and (v) recombination with ions left behind from previous pulses.

Experimentally, the measured fast pulses induced by electron movement have a typical duration of ≈ 1 ns and ion drift velocities are $\approx 10^{-3}$ times the electron ones, giving an estimated time of ≈ 1 μs to fully remove all charges from the gas gap. Because the typical repetition rates used in our setup do not exceed 20 Hz, the gas gap is completely emptied from all charges before a new pulse arrives, excluding effects (i) and (v) with ample margins.

From experimental investigations [5,6] and calculations [7] referring to typical RPC detector conditions (where electric field strengths are about twice the maximum value reached here), it is known that at some point the charge density inside the electron cloud is so high that its field starts to modify the externally applied one, effectively reducing the multiplication. It is important to note that such observations refer to atmospheric pressure, where the electron diffusion is small increasing the charge density in the electron cloud and hence the space charge field. In fact, at low pressures, transport parameters are routinely measured for E/N values even one order of magnitude higher than considered in the present work, without any significant side effect resulting from space charge [8,9]. Because some indications of space charge in pure isobutane have been found at atmospheric pressure [6] and nothing is known experimentally about the diffusion coefficients in this gas, rendering calculations difficult, the question is worth to be studied experimentally.

Measurements done with a cylindrical proportional counter employing a resistive glass cathode under X-ray irradiation [10,11] and with RPC cells exposed to gamma rays [12] have indicated the presence of an ohmic drop in the resistive electrode reducing the applied electric field. This conclusion depends, of course, on the resistance of the glass, the average charge produced per pulse and finally the repetition rate.

Recombination processes are well known to be present experimentally in the ionization chamber regime and they are responsible, for example, for the deviation of the response to light particles and to heavy ions from a simple scaling with ionization energy loss (also known as pulse-height-defect). A quantitative estimate is again rendered difficult by the lack of knowledge on the recombination and diffusion coefficients in pure isobutane.

A direct experimental approach has been followed in the present work. Three parameters are easily available to be changed in our setup: (i) the electric field strength (or more precisely the applied voltage), (ii) the laser beam intensity and (iii) the laser repetition rate. The dependence of each of the five effects on these three experimentally accessible quantities is summarized in Table 1. The most interesting feature to be observed is that these experimental parameters are not redundant and, if the full behavior of each of them is known, a mutually exclusive situation can be reached allowing to identify unambiguously the physical mechanism at work.

Table 1
Possible secondary processes in electron multiplication under uniform electric fields and their dependences on the parameters changed in the experiment.

	Electric field	Laser beam intensity	Laser repetition rate
Space charge (ionic comp.)	Increase	Linear prop.	Linear prop.
Space charge (el. comp.)	Increase	No effect	No effect
Ohmic drop	Increase	Linear prop.	Linear prop.
Recombination avalanche volume	Decrease	Quadratic	No effect
Recombination gas volume	Decrease	Quadratic	Quadratic

3. Experimental setup

Details on the experimental setup, mainly concerned with the mechanical construction and electronics, were given elsewhere [1,2]. A similar technique has also been employed by other groups [13,14]. Only few information relevant for what follows will be recalled. The cathode was made with an aluminum plate (40 mm diameter) and the anode consisted of a high resistivity (2×10^{12} Ω cm) glass slab of 3.5 mm thick and 32.5 mm× 32.5 mm area. The glass anode was glued on a brass plate (14 mm diameter) electrically insulated from the chamber by a piece of steatite 20 mm diameter and 30 mm long. The distance between the electrodes was adjusted by the means of micrometers and all measurements were carried out with 1.50 mm gas gap. High voltage was applied to the brass plate through a low-pass filter circuit (for details see Ref. [2]).

The primary electrons were liberated from the cathode by the incidence of a low divergence nitrogen laser beam (MNL200-LD LTB) with 337.1 nm wavelength. The beam has 1 mm × 2 mm dimensions, 700 ps pulse duration and nominal pulse energy of about 100 μJ at 15 Hz. The pulse repetition rate can be controlled and adjusted from 10 Hz up to 20 Hz via an interface with a PC. In order to perform measurements under different primary ionization conditions, the beam intensity was varied by using coverslips, calibrated to the laser wavelength, as attenuators. The average current was measured with an analogic electrometer Keithley 610C with accuracies of 2% and 4% of full scale on 0.3 to 10^{-11} A and on 3×10^{-12} to 10^{-14} A ranges, respectively. The capacitances involved in the circuit were chosen to meet the requirements of pulse current integration by the external chamber network for all laser repetition rates considered in the present study. All measurements were performed at room temperature (≈ 20 °C) and atmospheric pressure (≈ 940 hPa) in a flowing gas regime. Isobutane of 99.9% purity from Praxair was introduced in the chamber without further purification.

4. Results

The attention was focused on the first Townsend coefficient because it is the most sensitive transport parameter to any change in the electric field due to its exponential dependence. On the contrary, the drift velocity is almost saturated in the E/N

range below 200 Td (see Ref. [1]). As detailed in Ref. [2], it is advantageous to determine α/N by measuring the current growth, because any uncertainty in the drift velocity is not involved and the sensitivity to electronic noise is lower. The avalanche (I) and primary ionization (I_0) currents are measured and then α is obtained as $\ln(I/I_0)/d$ where d is the gas gap thickness. Despite this equation is derived from the Steady State Townsend (SST) technique, we have assumed that it holds to good approximation for pulsed irradiation of the cathode. A validation of this method with nitrogen, a very well-known gas, has been presented in our previous work [2].

Measurements of the first Townsend coefficient as a function of E/N in pure isobutane were performed within the range of 145−194 Td for different laser beam repetition rates and intensities (see Figs. 1 and 2). Considering that over the E/N range covered by this work there are no experimental values for pure isobutane available in the literature, to the best of our knowledge except for those of our previous paper, the results obtained were compared with those calculated by Magboltz 2 versions 7.1 and 8.6 [15–18]. Magboltz is a Monte Carlo code developed by S. Biagi to calculate electron transport parameters in the Steady State Townsend (SST) and Pulsed Townsend (PT) regimes simulating individual electron–atom collisions. The energy sharing in ionizing encounters between the original electron and the newly released one is parametrized with the Opal et al. [19] form. The anisotropy of the cross-sections can be included, if supported by the specific set used. Since Magboltz 2 version 8.2, the choice of the parametrization of the anisotropies is available between the form of Capitelli and Longo [20] (option 1) and the one of Okhrimovskyy et al. [21] (option 2). For the present discussion, Magboltz 2 version 7.1 and Magboltz 2 version 8.6 have been selected because they were available from our previous studies [1,2] and because they have different cross section sets for isobutane, namely "ISO 1999" and "ISO 2009", respectively. After "ISO 2009" no further development of the cross section set for isobutane has been done to the present date. The "ISO 1999" cross-section set is only isotropic, while "ISO 2009" allows the mentioned choices, but for simplicity only the isotropic case and option 2 are reproduced in Figs. 1 and 2. The lines are exactly the same as those presented in Fig. 4 of Ref. [2] and serve the main purpose of providing an immediate visual reference for the reader. It seems that the older cross-section set "ISO 1999" gives α/N values closer to our data. However, this is not the main focus of attention here. A careful comparison of the results for the two cross-section sets and for the parametrizations of the anisotropies in the "ISO 2009" case can be found in our previous work [2]. Their explanation or discussion will not be repeated here. The present data are fully consistent with those of Ref. [2]. The total uncertainties were estimated in 15% by comparing the results taken in several runs, at the same E/N, the same laser repetition rate and beam intensity.

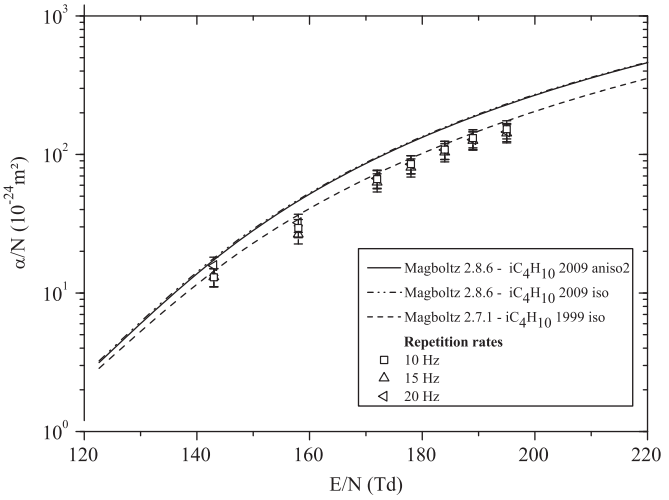

Fig. 1. First Townsend coefficient normalized to the gas density for i C_4H_{10} (isobutane). Magboltz results (continuous, dash dot and dashed lines, see text for details) and measured values with different laser beam repetition rates (square, triangle and side triangle).

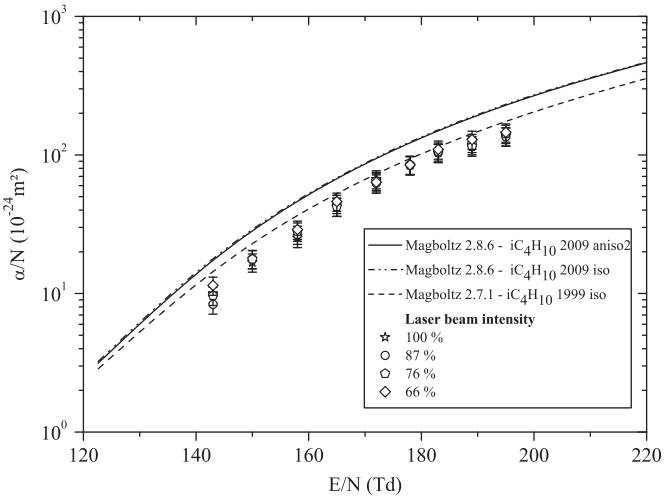

Fig. 2. First Townsend coefficient normalized to the gas density for i C_4H_{10} (isobutane). Magboltz results (continuous, dash dot and dashed lines, see text for details) and measured values with different attenuators at 20 Hz (star, circle, pentagon and lozenge).

Table 2
Values of the first Townsend coefficient α/N obtained with different laser repetition rates. Data are presented in Fig. 1. The total uncertainties were estimated to 15%. The E_{eff}/N columns refer to the effective E/N corrected for the ohmic drop across the glass anode as explained in the text.

Voltage V	E/N Td	E_{eff}/N Td 10 Hz	α/N 10^{-24} m^2	E_{eff}/N Td 15 Hz	α/N 10^{-24} m^2	E_{eff}/N Td 20 Hz	α/N 10^{-24} m^2
5000	143	143	13.0 ± 1.9	143	13.1 ± 2.0	143	15.8 ± 2.4
5500	158	158	29 ± 4	158	27 ± 4	158	32 ± 5
6000	172	172	66 ± 10	172	63 ± 9	172	67 ± 10
6200	178	177	85 ± 13	177	81 ± 12	177	85 ± 13
6400	184	183	108 ± 16	183	104 ± 16	182	108 ± 16
6600	189	187	131 ± 20	187	126 ± 19	187	128 ± 19
6800	195	191	152 ± 23	191	143 ± 21	190	146 ± 22

Even when repetition rates were varied from 10 to 20 Hz and the laser beam intensity was reduced in steps down to 66%, all the α/N values obtained by the current method agree, within the quoted uncertainty. To allow the reader to better assess the quantitative agreement between the different cases, the data of Figs. 1 and 2 are also reproduced in Tables 2 and 3, respectively.

5. Discussion of the results

In the E/N range examined here, the agreement between the values obtained for α/N with different laser repetition rates and laser intensities exclude an important presence of secondary processes. This is very reassuring because it validates the results presented here and in the previous publications [1,2]. While, as mentioned in Section 2, the absence of a contribution from ions left behind from previous pulses can be expected, the same conclusion is not so obvious for the electron space charge. In fact, according to

Table 3
Values of the first Townsend coefficient α/N obtained with different laser intensities. Data are presented in Fig. 2. The repetition rate was 20 Hz. The total uncertainties were estimated to 15%. The E_{eff}/N columns refer to the effective E/N corrected for the ohmic drop across the glass anode as explained in the text.

Voltage V	E/N Td	E_{eff}/N Td 100%	α/N 10^{-24} m^2	E_{eff}/N Td 87%	α/N 10^{-24} m^2	E_{eff}/N Td 76%	α/N 10^{-24} m^2	E_{eff}/N Td 66%	α/N 10^{-24} m^2
5000	143	143	10.0 ± 1.5	143	8.4 ± 1.3	143	9.6 ± 1.4	143	11.4 ± 1.7
5250	150	150	17 ± 3	150	18 ± 3	150	18 ± 3		
5500	158	158	25 ± 4	158	27 ± 4	158	28 ± 4	158	29 ± 4
5750	165	165	42 ± 6	165	44 ± 7	165	42 ± 6	165	46 ± 7
6000	172	172	66 ± 10	172	62 ± 9	172	65 ± 10	172	64 ± 10
6200	178	177	84 ± 13	177	85 ± 13	177	84 ± 13	177	85 ± 13
6400	183	181	103 ± 15	182	103 ± 16	182	106 ± 16	182	110 ± 16
6600	189	186	116 ± 17	185	122 ± 18	187	115 ± 17	187	129 ± 19
6800	195	188	136 ± 20	189	136 ± 20	190	142 ± 21	191	145 ± 22

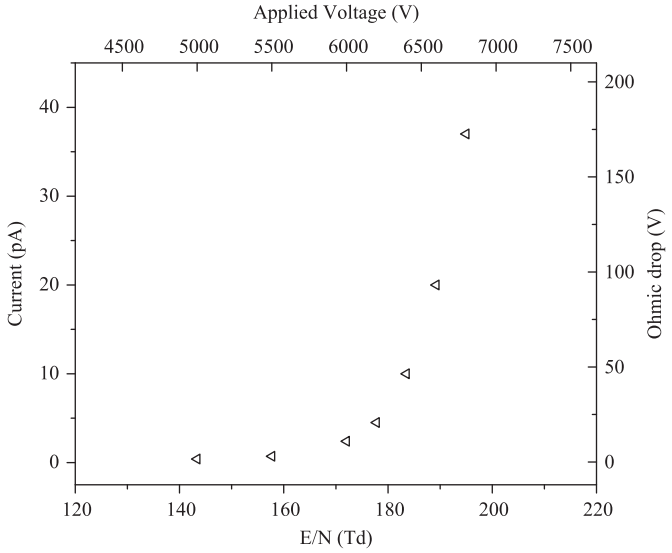

Fig. 3. Ohmic drop across the glass anode corresponding to the measured current at the nominal laser beam intensity and the maximum repetition rate of 20 Hz. The other values assumed in this calculation are described in the text.

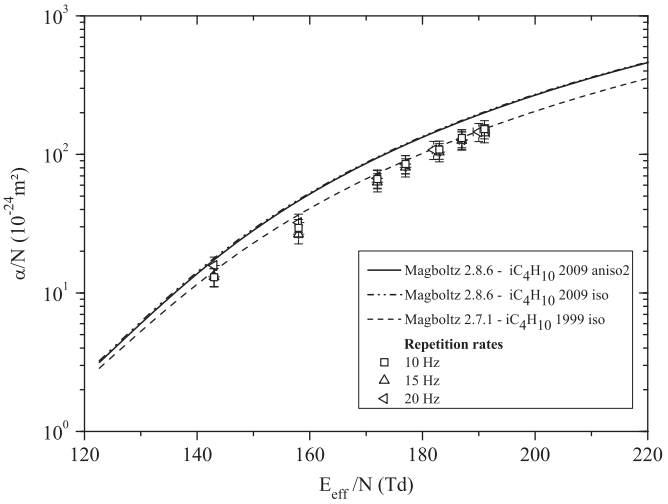

Fig. 4. First Townsend coefficient normalized to the gas density for i C_4H_{10} (isobutane). Magboltz results (continuous, dash dot and dashed lines, see text for details) and measured values with different laser beam repetition rates (square, triangle and side triangle). The E/N values have been corrected for the ohmic drop across the glass anode to obtain an effective E_{eff}/N as explained in the text.

Ref. [6], when E/N will be gradually extended, the electron space charge has to become important. These cross-checks will have to be repeated in the future and might possibly set an ultimate limit to the highest E/N which can be covered at atmospheric pressure without important distortions.

The ohmic drop can be calculated from the measured current across the gap and the resistivity of the anode glass ($2 \times 10^{12}\ \Omega$ cm), once the area of the laser beam projected onto the cathode is known. To this end, a foil of millimetric paper was overlaid on the electrode keeping the same geometric configuration used in the measurements. In particular, the inclination of the beam necessary to enter the gap has been accurately reproduced. The projected spot had dimensions of 3×5 mm^2. In Fig. 3 the measured current and the calculated ohmic drop across the anode (right vertical scale) are depicted in the worst possible case of the full nominal laser intensity and the highest repetition rate of 20 Hz. For comparison, the applied voltage is given in the upper horizontal scale of the same figure. The correction to the applied voltage reaches $\approx 2.5\%$ in the last point and is not completely negligible. For this reason, Figs. 4 and 5 show the same data of Figs. 1 and 2, but now with an effective E_{eff}/N value, calculated from the voltage across the gap corrected for the ohmic drop. The same information is also included in Tables 2 and 3 with an extra column (labelled E_{eff}/N). The resistivity of the glass ρ depends on its temperature, which is not controlled in our setup. Using the

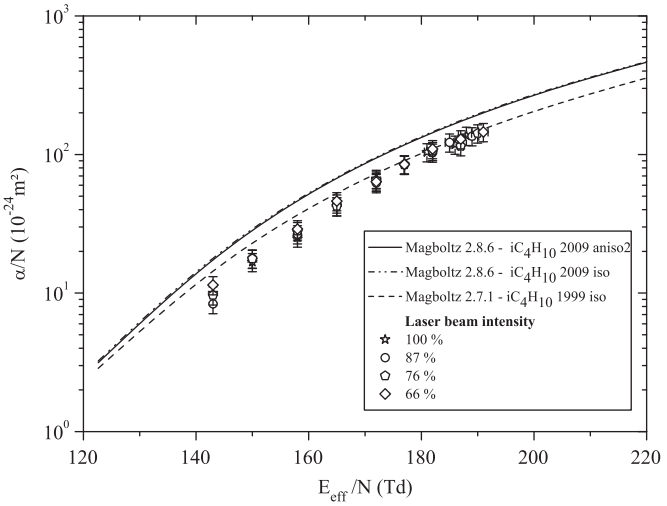

Fig. 5. First Townsend coefficient normalized to the gas density for i C_4H_{10} (isobutane). Magboltz results (continuous, dash dot and dashed lines, see text for details) and measured values with different attenuators at 20 Hz (star, circle, pentagon and lozenge). The E/N values have been corrected for the ohmic drop across the glass anode to obtain an effective E_{eff}/N as explained in the text.

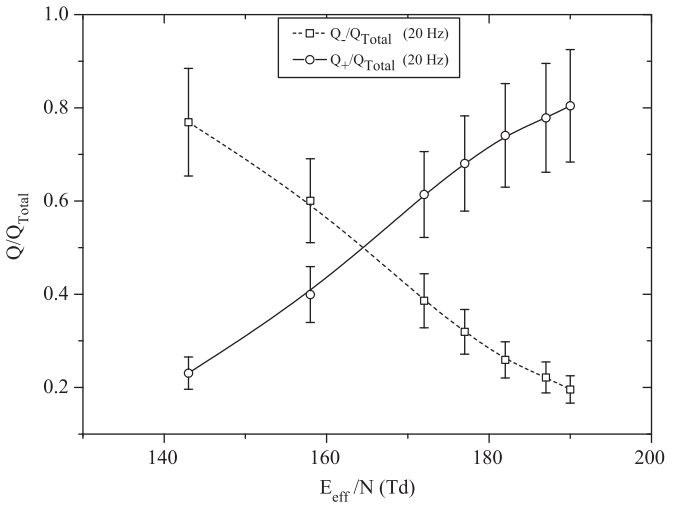

Fig. 6. Ionic (circle) and electronic (square) contribution to the total induced charge at 20 Hz. The smooth line is intended only to guide the eye.

measured values of this dependence for various types of glass (see Table 1 of Ref. [22]) and considering a typical temperature variation of $\approx \pm 2$ °C, a corresponding change in ρ of $\approx 20\%$ is estimated. The latter uncertainty on ρ dominates over the measurement error on ρ and on the current. Because the correction grows with the ohmic drop, the error remains negligible but, on the last point, where it is indicated with an horizontal bar (almost the size of the symbols) in Figs. 4 and 5. It is clearly visible that the saturation of α apparent at the highest values of E/N in Figs. 1 and 2 has been fully removed in Figs. 4 and 5. Hence, once the effect of the ohmic drop has been corrected away, α/N continues to grow with E_{eff}/N like in the Magboltz 2 simulation.

From the classical theory of current growth in gases, the components due to electrons Q_- (or ions Q_+) of the total induced charge Q_{Total} are related to the first Townsend coefficient and the avalanche length [23,24]. In the present configuration, the initial electrons are released from the cathode, hence the avalanche length is just the gap d between the electrodes. Then, neglecting secondary ionization processes, the classical formulae can be rewritten as

$$\begin{cases} \dfrac{Q_-}{Q_{\mathrm{Total}}} = \dfrac{1-e^{-\alpha d}}{\alpha d} \\ \dfrac{Q_+}{Q_{\mathrm{Total}}} = \dfrac{\alpha d + e^{-\alpha d} - 1}{\alpha d} \end{cases} \quad (1)$$

By using the values of α obtained in this work, Q_-/Q_{Total} and Q_+/Q_{Total} can be calculated as a function of E_{eff}/N and are reported in Fig. 6. For E_{eff}/N higher than 165 Td, the main cause of induction is the movement of positive ions. As a consequence of the agreement among the α/N values, these calculations are not affected by the laser repetition rate and the beam intensity, so that only one case is reproduced in Fig. 6.

6. Conclusions

In this work, the investigation of the possible limitations present in our dedicated setup to measure electron transport parameters has been carried one step forward, excluding the presence of secondary processes in the E/N range covered so far, except for the ohmic drop across the resistive anode toward the last points. This effect has been corrected for. Such conclusions are based on a study of the stability of the results (in particular the first Townsend coefficient, the most sensitive transport parameter to even a modest variation in the electric field uniformity) with the laser repetition rate and beam intensity.

As a main result interesting to a broader community, the determination of the first Townsend coefficient contained in the previous paper has been fully validated. It is made available here in tabular form.

Acknowledgements

The authors are deeply grateful to Eng. J.S. Nascimento for his support concerning the high voltage system and the signal readout electronics. They thank Dr. M.M.R. Fraga for helpful discussions on the possible limitations of our setup and for her continuous encouragement. A. Mangiarotti acknowledges two fellowships from FAPESP (contracts 07/50591-4 and 09/51809-9). I.B. Lima and T.C. Vivaldini would like to thank CNPq for the award of scholarships. This work was co-financed by FAPESP under contract 02/04697-1, by CNPq via contracts 478859/2009-0 and 479079/2010-2.

References

[1] P. Fonte, A. Mangiarotti, S. Botelho, J.A.C. Gonçalves, M.A. Ridenti, C.C. Bueno, Nuclear Instruments and Methods A 613 (2010) 40.
[2] I.B. Lima, A. Mangiarotti, T.C. Vivaldini, J.A.C. Gonçalves, S. Botelho, P. Fonte, J. Takahashi, L.V. Tarelho, C.C. Bueno, Nuclear Instruments and Methods A 670 (2012) 55.
[3] A. Mangiarotti, A Theoretical Study of the Fast Signal Induced by Avalanche Growth in Pure Nitrogen and Pure Isobutane, Activity Report of Project FAPESP 07/50591-4.
[4] I. Krajcar Bronić, B. Grosswendt, Nuclear Instruments and Methods B 142 (1998) 219.
[5] R. Cardarelli, V. Makeev, R. Santonico, Nuclear Instruments and Methods A 382 (1996) 470.
[6] P. Fonte, V. Peskov, Nuclear Instruments and Methods A 477 (2002) 17.
[7] C. Lippmann, W. Riegler, Nuclear Instruments and Methods A 533 (2004) 11.
[8] M.A. Folkard, S.C. Haydon, Journal of Physics B 6 (1973) 214.
[9] S.C. Haydon, O.M. Williams, Journal of Physics D 9 (1976) 523.
[10] C.C. Bueno, M.M. Fraga, J.A.C. Gonçalves, R. Ferreira Marques, A.J.P.L. Policarpo, M. Damy de S. Santos, Nuclear Instruments and Methods A 408 (1998) 496.
[11] M.M. Fraga, R. Ferreira Marques, Y. Ivaniouchenkov, E.P. de Lima, F. Neves, A.J.P.L. Policarpo, C.C. Bueno, J.A.C. Gonçalves, M. Damy de S. Santos, L. Costa, S. Mendiratta, J.H. Monteiro, Nuclear Instruments and Methods A 419 (1998) 485.
[12] G. Aielli, P. Camarri, R. Cardarelli, A.D. Ciaccio, L.D. Stante, B. Liberti, A. Paoloni, R. Santonico, Nuclear Instruments and Methods A 456 (2000) 82.
[13] P. Colas, A. Delbart, J. Derré, I. Giomataris, F. Jeanneau, V. Lepeltier, I. Papadopoulos, P. Rebourgeard, Nuclear Instruments and Methods A 478 (2002) 215.
[14] G. Chiodini, M. Colucci, E. Gorini, M. Primavera, S. Stella, Nuclear Physics B (Proceedings Supplements) 158 (2006) 133.
[15] S. Biagi, Nuclear Instruments and Methods A 273 (1988) 533.
[16] S. Biagi, Nuclear Instruments and Methods A 283 (1989) 716.
[17] S. Biagi, Nuclear Instruments and Methods A 421 (1999) 234.
[18] S. Biagi, Magboltz, the Fortran source code of the stand alone version is freely downloadable from 〈http://consult.cern.ch/writeup/magboltz/〉 (2007).
[19] C.B. Opal, W.K. Peterson, E.C. Beaty, Journal of Physical Chemistry 55 (1971) 4100.
[20] S. Longo, M. Capitelli, Plasma Chemistry and Plasma Processing 4 (1994) 1.
[21] A. Okhrimovskyy, A. Bogaerts, R. Gijbels, Physical Review E 65 (2002) 037402.
[22] D. González-Díaz, D. Belver, A. Blanco, R. Ferreira Marques, P. Fonte, J. Garzón, L. Lopes, A. Mangiarotti, J. Marín, Nuclear Instruments and Methods A 555 (2005) 72.
[23] H. Raether, Electron Avalanches and Breakdown in Gases, Butterworths, 1964.
[24] G.G. Raju, Gaseus Electronics, Theory and Practice, CRC—Taylor and Francis Group, 2006.